

Response spectrum analysis for regular base isolated buildings subjected to near fault ground motions

Leblouba Moussa*

Curtin University, Sarawak Campus, CDT 250, 98009 Miri, Sarawak, Malaysia

(Received March 30, 2011, Revised May 28, 2012, Accepted August 7, 2012)

Abstract. This paper presents a response spectrum analysis procedure suitable for base isolated regular buildings subjected to near fault ground motions. This procedure is based on the fact that the isolation system may be treated separately since the superstructure behaves as a rigid body on well selected isolation systems. The base isolated building is decomposed into several single-degree of freedom systems, the first one having the total weight of the building is isolated while the remainder when superposed they replicate approximately the behavior of the superstructure. The response of the isolation system is governed by a response spectrum generated for a single isolated mass. The concept of the procedure and its application for the analysis of base isolated structures is illustrated with an example. The present analysis procedure is shown to be accurate enough for the preliminary design and overcomes the limits of applicability of the conventional linear response spectrum analysis.

Keywords: response spectrum; base isolation; building; isolation system

1. Introduction

The effectiveness of the base isolation technique has been demonstrated through the performance of several base isolated structures during destructive earthquake events. A good example is the successful performance of the base isolated University of Southern California (USC) hospital building during the Northridge earthquake of 17 January 1994 (Çelebi 1996). The isolation system at the base of a structure deflects the seismic energy so that it will not be transferred to the superstructure. The benefits gained by using such technique are substantial and can be itemized after Stanton and Roeder (1991) as:

- Reduced floor accelerations and interstory drifts;
- Reduced (or no) damage to structural elements;
- Better protection of buildings contents;
- Concentration of nonlinear, large deformation behavior into one group of elements (the isolation bearings and dampers).

The last item highlights an important inherent property of a well selected and designed isolation system. The superstructure may remain elastic under these conditions and most deformations occur at the isolation level, thus the expensive contents and equipment in base isolated structures remain

*Corresponding author, Ph.D., E-mail: moussa@curtin.edu.my

intact from minim damages. However, the challenge is how to select the appropriate isolation system parameters. Several design and analysis methods were proposed, but a common problem arise in the complexity of implementation that require an extensive effort to be performed. Therefore, we are interested in developing simple but efficient procedures that lead to an appropriate design with minimum effort. Most isolators behave beyond the inelastic range; however, some of them may be modeled using equivalent linear models such as elastomeric bearings (EB). Chopra (2005) demonstrated the benefits of seismic isolation technique using conventional response spectrum analysis (RSA). Ribakov (2010) introduced and investigated the performance of a hybrid seismic isolation system with passive variable friction dampers against near fault earthquakes, where the system consisted of replacing the conventional column fixed to the foundations by seismic isolation ones. However, the Lead Rubber Bearing (LRB) and Friction Pendulum system (FPS) are the widely used seismic isolators.

Nagarajaiah *et al.* (1991) developed an analytical model and a solution algorithm for nonlinear dynamic analysis of three-dimensional base isolated structures with elastomeric and sliding isolation systems where nonlinear behavior is restricted to the base and the superstructure is considered to be elastic at all times, the algorithm has been implemented in a computer program called 3D-BASIS (Nagarajaiah *et al.* 1991, 1994). Deb *et al.* (1997) developed a simplified nonlinear dynamic analysis of base isolated buildings subjected to general plane motion based on a simple close form solution of the stiff differential equations of hysteretic model for force mobilized in the nonlinear elements of the base isolator system. Nagarajaiah *et al.* (1993) evaluated the torsional coupling in elastomeric base-isolated structures, and concluded that the total superstructure response reduces significantly due to the effects of the elastomeric base isolation and torsional amplification can be significant depending on the isolation and superstructure eccentricity and the lateral and torsional flexibility. Jangid and Kelly (2001) conducted a comparative study on the performance of four isolation systems subjected to normal component of selected near fault ground motions, they found that EDF type isolation systems may be the optimum choice for the design of isolated structures in near-fault locations. Later, Jangid (2007) evaluated the response of multistory shear type flexible buildings isolated by lead-rubber bearings (LRB) subjected to near fault ground motions, where he concluded that for low bearing yield strength there is significant displacement in the bearing and the optimum yield strength of the LRB is found to be in the range of 10-15% of the total weight of the structure. Seguíñ *et al.* (2008) investigated the linear earthquake response of seismically isolated structures with lateral torsional coupling, where two simplified procedures for estimating the amplification of edge displacements of the superstructure and isolated base; the first model accounts for the base-superstructure interaction through a correction of the mass matrix of the superstructure, while the second assumes a pseudo-static response of the superstructure subjected to three lateral inertial force distributions.

Studies performed by Vasant and Jangid (2004) concluded that the equivalent linear elastic-viscous damping model for a bilinear hysteretic model of the isolator underestimates the superstructure acceleration and overestimates the bearing displacement, and a significant difference in the frequency content of superstructure acceleration of base isolated structure predicted by the equivalent linear and bilinear isolator models. Ryan and Chopra (2004) demonstrated that the equivalent linear procedures in building codes were shown to underestimate the isolator deformation by 20-50% compared to the median deformation determined by nonlinear response history analysis.

Due to the inaccuracy of formulations in building codes, several researchers (Andriono and Carr 1991, Lee *et al.* 2001, Tsai *et al.* 2003, Tsai *et al.* 2006, York and Ryan 2008, Cardone *et al.* 2009)

Table 1 Proposed vertical distributions of equivalent static forces (values of s_i)

Author	s_i	Definitions
Andriono and Carr (1991a, b)	h_i^p	h_i : Height of the story i ; p : Function of the nonlinearity factor (NL) and the fundamental period of the un-isolated building (T_{1UI}).
Lee <i>et al.</i> (2001)	$1 + \frac{\varepsilon}{0.6H} h_i$	$\varepsilon = \frac{\omega_b^2}{\omega_s^2}$; ω_b : Circular frequency of the base isolated building; ω_s : Circular frequency of the fixed base building; H : Total height of the superstructure.
Tsai <i>et al.</i> (2003)	$1 + \frac{\varepsilon}{H} h_i$	//
York and Ryan (2008)	h_i^k	$k = 11.21 \xi^{1.155} T_{1UI}^{0.889}$; A concentrated force $F_t = 0.425 \xi^{0.66} T_{1UI}^{0.724}$ is added to the top floor level.
Cardone <i>et al.</i> (2009)	Δ_i	Δ_i : Story displacement, calculated by linear combination of the first three mode shapes of the base isolated building.

proposed different approaches to determine the vertical distribution of equivalent static forces throughout the height of base isolated buildings. The proposed distributions can be expressed in the following code-type form

$$F_i = V_b \frac{m_i s_i}{\sum m_j s_j}$$

where F_i , V_b and m_i are the story forces, base shear, and story masses, respectively. Table 1 summarizes the expressions for s_i proposed by different authors.

Andriono and Carr (1991a, b) found the exponent p to be strongly correlated to the nonlinearity factor, NL and the fundamental period of vibration of the un-isolated building, T_{1UI} , but they didn't express explicitly this correlation. Similar formulation has been proposed by York and Ryan (2008), however, to limit the exponent k to lower values and to better preserve the overall shape of the vertical distribution of forces, York and Ryan (2008) suggested an additional concentrated force F_t at the roof level. Both the exponent k and F_t are expressed based on regression analysis, as a function of the effective damping, ξ and T_{1UI} (Table 1).

Distributions proposed by Lee *et al.* (2001) and Tsai *et al.* (2003) are very similar and take into account the influence of the first mode of vibration of the base isolated structure. Such distributions do not properly account for nonlinear response behavior of the isolation system, nor the higher modes effect. To obtain accurate vertical force distribution Tsai *et al.* (2006) proposed more complicated design formula to overcome the limits of the formulation proposed before by the same authors (Tsai *et al.* 2003). In the new formula the higher modes effect is accounted for by taking into account the influence of the first two modes of vibration of the base isolated structure and the higher mode contributions of the structure.

Recently, Cardone *et al.* (2009) have developed an alternative vertical distribution of equivalent static forces (3M-Method) using floor displacements ($s_i = \Delta_i$). The displacement profile Δ_i is

expressed as a linear combination of the first three mode shapes of the base isolated building. The disadvantage of the 3M-Method is in the determination of the combination coefficients of the mode shapes, which is based on charts generated using limited data rather than a general expression that is valid for wider range of isolation systems and buildings.

In this paper a response spectrum analysis procedure for base isolated symmetric buildings (RSA-BI) is developed. This procedure is based on a response spectrum for base isolated structures (called in this paper Seismic Isolation Response Spectrum, SIRS), and benefits from the aforementioned features of isolation systems. Zayas *et al.* (1989) initiated the idea of construction of the SIRS for friction pendulum system (FPS), and based on the fact that the estimated deformation based on nonlinear analysis for a single ground motion, such as demonstrated in Makris and Chang (2000) would be sensitive to the particular ground motion used, Ryan and Chopra (2004, 2005, 2006) developed an earthquake spectra that gives a normalized deformation insensitive to ground motion intensity. In the construction of the earthquake spectra, the ground motions selected by Ryan and Chopra (2004, 2005, 2006) were normalized with respect to the peak ground velocity (PGV) since base isolated structures fall always in the velocity and displacement sensitive regions of the spectrum. The constant strength design spectrum (CSDS) (Tena-Colunga 2002) is basically a modification of the modified response spectrum proposed by Newmark and Hall (1982), where the normalized yield strength (yield strength over the weight) of a single degree of freedom system is fixed rather than the displacement ductility factor. The CSDS can be constructed for bilinear systems with a given yield strength and postyield stiffness. The RSA-BI method helps in the analysis as well as in the design stage and may replace the conventional RSA. Presented first is the procedure of construction of the SIRS then the procedure of RSA-BI is developed. Finally, the response of a six-story asymmetric building example demonstrates the application of the proposed procedure, and results are compared with the results obtained by the nonlinear time history analysis of the three-dimensional base isolated structure.

2. Seismic isolation response spectra

It has been found that structural periods and damping ratios (above the isolation level) have no significant effect on the peak response of base isolated structures (Jangid 2002, Moussa 2009, among others) since the isolation period is much longer than the first structural period and the damping provided by the isolation system through its inherent hysteretic property is much greater than the structural damping. Ryan and Chopra (2004, 2005) constructed a design spectrum for LMSR suite of ground motions based on nonlinear RHA for a given number of design parameters, they assumed that the preyield (elastic) stiffness has no effect (Makris and Chang 2000) then using a constant yield displacement $x_y = 1$ cm for LRB is reasonable. Based on the Bouc-Wen model (Park 1986, Wen 1976) instead of bilinear approximation, in what follows we summarize the procedure of construction of the seismic isolation response spectrum (SIRS) for LRB and Friction Pendulum System (FPS) that will be needed for the RSA-BI. Details on the construction of SIRS for an ensemble of ground motions can be found in Ryan and Chopra (2004, 2005).

2.1 Lead rubber bearing

Considering a single mass mounted on an isolation system consists of LRB as depicted in Fig. 1.

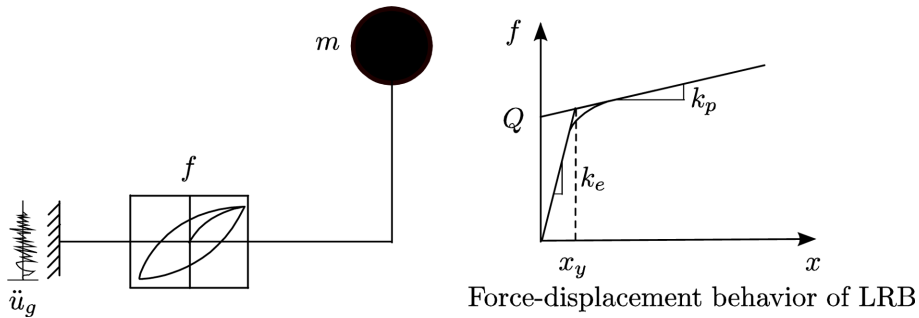


Fig. 1 Single isolated mass with LRB

The isolation system is modeled using the Bouc-Wen model (Park 1986, Wen 1976) characterized by the dimensionless z .

The equation of motion of the system mass-seismic isolation is

$$m\ddot{x} + f = -m\ddot{u}_g(t) \quad (1)$$

The mobilized force f in the LRB is given by

$$f = k_p x + (k_e - k_p)x_y z \quad \text{or simply} \quad f = k_p x + Qz \quad (2)$$

Where k_e , k_p , and Q are the preyield stiffness, postyield stiffness and the yield strength of LRB, respectively. The dimensionless z , which characterizes the Bouc-Wen model for unidirectional motion is given by Park (1986), Wen (1976)

$$\dot{z} = \frac{\dot{x}}{x_y} [A - |z|^n (\gamma \text{sign}(\dot{x}z) + \beta)] \quad (3)$$

Eq. (1) can be written at the following form

$$\ddot{\bar{x}} + \omega_b^2 \bar{x} + \omega_b^2 z = -\omega_b^2 \frac{\ddot{u}_{g0}(t)}{\mu} \quad (4)$$

in which, μ represents the yield strength to total weight ratio, $\ddot{u}_{g0}(t) = \ddot{u}_g(t)/g$ and g is the gravity, and $\bar{x} = x\omega_b^2/\mu g$ is the normalized displacement. Parameters A , β , γ , and n that control the shape of the hysteretic loop can be taken as (Reinhorn *et al.* 1995): $A = 1$, $\beta = 0.1$, $\gamma = 0.9$, and $n = 2$. Solving Eq. (4) for several values of μ and T_b one can construct a response spectrum (SIRS) for a particular earthquake or an ensemble of ground motions (Ryan and Chopra 2004, 2005) that gives the peak-normalized displacement.

Fig. 2 shows the SIRS for El Centro 1940 ($PGA = 0.319$ g, $PGV = 37.14$ m, $PGD = 21.34$ m) for LRB isolation system, where $x_y = 1$ is considered (Ryan *et al.* 2004, 2005). If the SIRS for a given ground motion component or an ensemble of ground motions is available, the peak value of deformation or of the base shear for any base isolated structure can be determined readily. This is the case because the computationally intensive nonlinear dynamic time history analyses have already been completed in generating the spectrum. Corresponding to the pair (T_b, μ) , the value of \bar{x} is read from the SIRS. Then, the peak isolation deformation x_b can easily be determined by

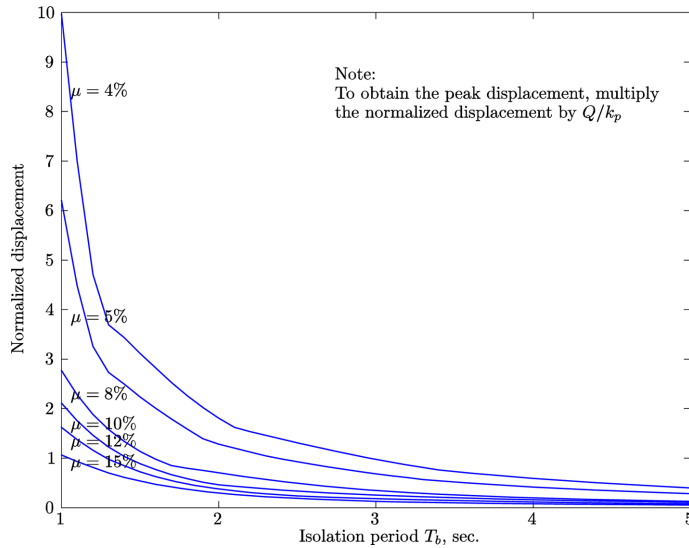


Fig. 2 SIRS for LRB (El Centro 1940 NS Component), $x_y = 1 \text{ cm}$

multiplying \bar{x} by Q/k_p . The base shear of the structure is given by Eq. (2). It is possible to estimate the maximum base shear from the SIRS assuming $z = 1$ (z is bounded by -1 and $+1$)

$$V_b \approx k_p x_b + Q \quad \text{or simply} \quad V_b \approx \mu W(1 + \bar{x}) \tag{5}$$

Better approximation of the dimensionless z can be obtained using the following equation (Moussa 2009)

$$z = 1 - \exp(-x_b/x_y) \tag{6}$$

Eq. (6) was obtained by solving Eq. (3) assuming $n = 1$ and an increased positive displacement to a single isolated mass.

2.2 Friction pendulum system (FPS)

As done for the LRB, we will achieve at the same system of equations to be solved numerically to construct the SIRS for FPS, the only difference is in the physical meaning of μ . For the friction pendulum isolation system, μ is the coefficient of sliding friction at sliding velocity which may be approximated by the following equation (Mokha 1988)

$$\mu = f_{\max} - \Delta f \exp(-a|\dot{x}|) \tag{7}$$

in which f_{\max} is the coefficient of friction at large velocity of sliding and Δf is the difference between f_{\max} and the sliding value at very low velocity, and a is a constant for given bearing pressure and condition of interface.

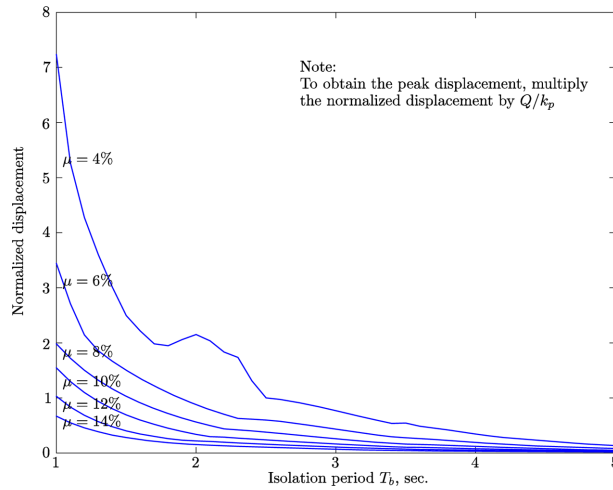


Fig. 3 SIRS for FPS (El Centro 1940 NS Component), $x_y = 0.127$ cm

The isolation period is related only to the radius of curvature of the spherical sliding surface R

$$T_b = 2\pi \sqrt{\frac{R}{g}} \quad \text{and} \quad R = \frac{T_b^2 g}{4\pi^2} \quad (8)$$

A yield displacement of 0.127 cm is used in the construction of the SIRS for El Centro 1940 for FP isolation system shown in Fig. 3.

3. Response spectrum analysis of base isolated buildings (RSA-BI)

For an MDOF system isolated at its base, the matrix form of differential equations governing its response to earthquake induced ground motion is (Nagarajaiah *et al.* 1991, Reinhorn *et al.* 1994, Narasimhan *et al.* 2003)

$$\text{Superstructure: } M_s \ddot{U} + C_s \dot{U} + K_s U = -Mr(\ddot{u}_g(t) + \ddot{x}) \quad (9)$$

$$\text{Base isolation: } r^T M_s [\ddot{U} + r(\ddot{u}_g(t) + \ddot{x})] + m_b(\ddot{u}_g(t) + \ddot{x}) + f = 0 \quad (10)$$

Where M_s and K_s are the mass and stiffness matrices of the superstructure, r is the vector of earthquake influence coefficients. The damping matrix C_s would not be needed.

As aforementioned, the idealization of a base isolated structure as a block mass mounted on isolation system is reasonable since the resulted peak responses are accurate. For this and as a reasonable approximation, we neglect the term containing any structural response quantity from Eq. (10), which are in this case the floor accelerations relative to the base. In fact, the above equations of motion are weakly coupled. Therefore, Eq. (10) collapses to an equation of motion of a single isolated mass M_{tot} (the total mass of the building including the base)

$$\ddot{x} + \frac{f}{M_{tot}} = -\ddot{u}_g(t) \quad (11)$$

Eq. (11) is similar to Eq. (1). Seguín *et al.* (2008) used the same approximation to develop the Mass-Correction Model (MCM), however, their modeling is restricted to linearly isolated structures.

The base isolated MDOF system can be decomposed into simple SDF systems, the first one is isolated having the total mass of the building including the base while the remainder when superposed they constitute the superstructure. While the SIRS has been used to determine the peak base displacement and maximum base shear, another response spectrum is needed for determination of peak modal responses for the superstructure; this response spectrum is constructed by solving a SDF system (for a wide range of natural periods and damping ratios) fixed at its base, subjected to the excitation $(\ddot{u}_g(t) + \ddot{x})$ (see Eq. (9) and this requires solving Eq. (11) several times to provide the base acceleration for every isolation system parameters (several pairs of T_b and μ). However, the construction of such spectrum can be avoided using the technique described next and by taking into account that the superstructure damping ratios have no effect on the peak response so that they can be neglected. From Eq. (11)

$$\max|\ddot{x} + \ddot{u}_g(t)| = \max\left|\frac{f}{M_{tot}}\right| = \frac{1}{M_{tot}}\max|f| \quad (12)$$

The base shear is determined using Eq. (5) and the maximum absolute value of the total acceleration of the base, $\max|\ddot{x} + \ddot{u}_g(t)|$ is calculated using Eq. (12). The peak modal responses for the superstructure are calculated by static analysis of each SDF system subjected to the pseudo-acceleration, ps_a defined by

$$ps_a = \frac{V_b}{M_{tot}} \quad (13)$$

The procedure to compute the peak response of an N story base isolated building (N stories + base) to earthquake ground motion characterized by a seismic isolation response spectrum (SIRS) is summarized in step-by-step form:

1. Define M_{str} and K_{str} , the mass and lateral stiffness matrices of the structure (including the base);
2. Determine the natural frequencies ω_i and natural modes of vibration ϕ_i of the structure (base included). For the superstructure, the spectral matrix, Ω_{sup}^2 and the modal matrix, Ω_{sup} are determined from Ω^2 , the spectral matrix of the structure, and from Φ , the modal matrix of the structure including the base, respectively, this is illustrated in Fig. 4.
3. Determine the isolation system parameters: the yield strength to the total weight ratio μ and the postyield stiffness k_p ;
4. Corresponding to the isolation period T_b and yield strength to total weight ratio μ , read the normalized base displacement from the SIRS and compute the peak base displacement x_b (see section 2);
5. Compute the maximum base shear from Eq. (5) or Eq. (2) and Eq. (6);
6. Compute the peak response in the i th mode by the following steps to be repeated for all modes:
 - a) Corresponding to natural period T_b , compute the deformation D_i from the following equation:

$$D_i = \frac{ps_a}{\omega_i^2}$$

Note that the total mass M_{tot} used in Eq. (13) is to be recalculated because the isolation period T_b defined in step 2 is different from that computed using k_p and M_{tot} , so:

$$M_{tot}^* = \frac{k_p}{\omega_b^2}$$

b) The pseudo-acceleration is constant for all structural modes:

$$\ddot{D}_i = 1 \cdot p s_a \quad (m_i = 1, \text{ unit mass SDF systems})$$

c) Compute the modal floor displacements relative to the base, u_{ji} using the following equation:

$$u_{ji} = \Gamma_i \phi_{sup i} D_i$$

where Γ_i is the modal participation factor described by the following equation:

$$\Gamma_i = \frac{\phi_{sup i}^T M_s r}{\phi_{sup i}^T M_s \phi_{sup i}}$$

d) Compute the equivalent static lateral forces f_{ji} using the following equation:

$$f_{ji} = \Gamma_i m_j \phi_{sup i} \ddot{D}_i$$

e) Compute the story forces -shear and moments- and element forces -bending moments and shears- by static analysis of the structure subjected to lateral forces f_i ;

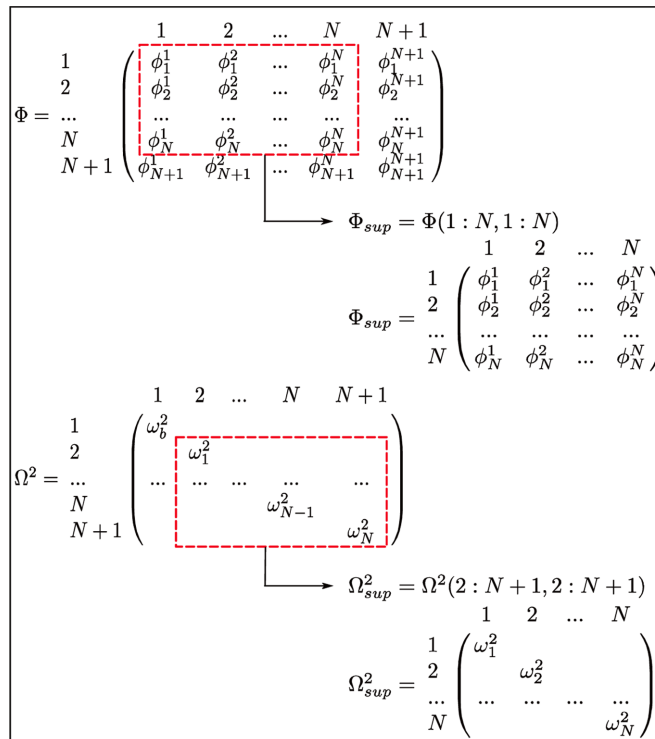


Fig. 4 Determination of Φ_{sup} and Ω_{sup}^2 corresponding to the superstructure

7. Finally,

- Determine and estimate the peak floor displacements using the SRSS technique of superposition, then add the base displacement calculated at step 4 to the floor displacements u_j to get the peak floor displacements x_j relative to the ground;
- SRSS the forces f_j to get the peak floor forces. For shear forces use the same technique.

4. Verification example

The analysis of a six-story reinforced concrete base isolated structure with LRB isolation system is considered. The 3D, plan and elevation views are shown in Fig. 5. The reinforced concrete superstructure is designed to resist lateral loads using column elements. The vertical axis of centers of mass is offset from the geometric center of the structure, inducing a mass eccentricity of 17 cm in the Y direction. The uncoupled translational period of the superstructure $T_s = 0.64$ sec. in both X and Y directions for a complete three-dimensional representation and $T_s = 0.39$ sec. in both X and Y directions for a three-dimensional shear representation assuming rigid floors. A value of 5% of critical damping is used for the superstructure in all modes.

The LRB isolation system was designed based on practical parameters. The average isolation yield strength Q_y is set to $5\%W$, where W is the total weight of the structure $W = 13560.47$ kN. The

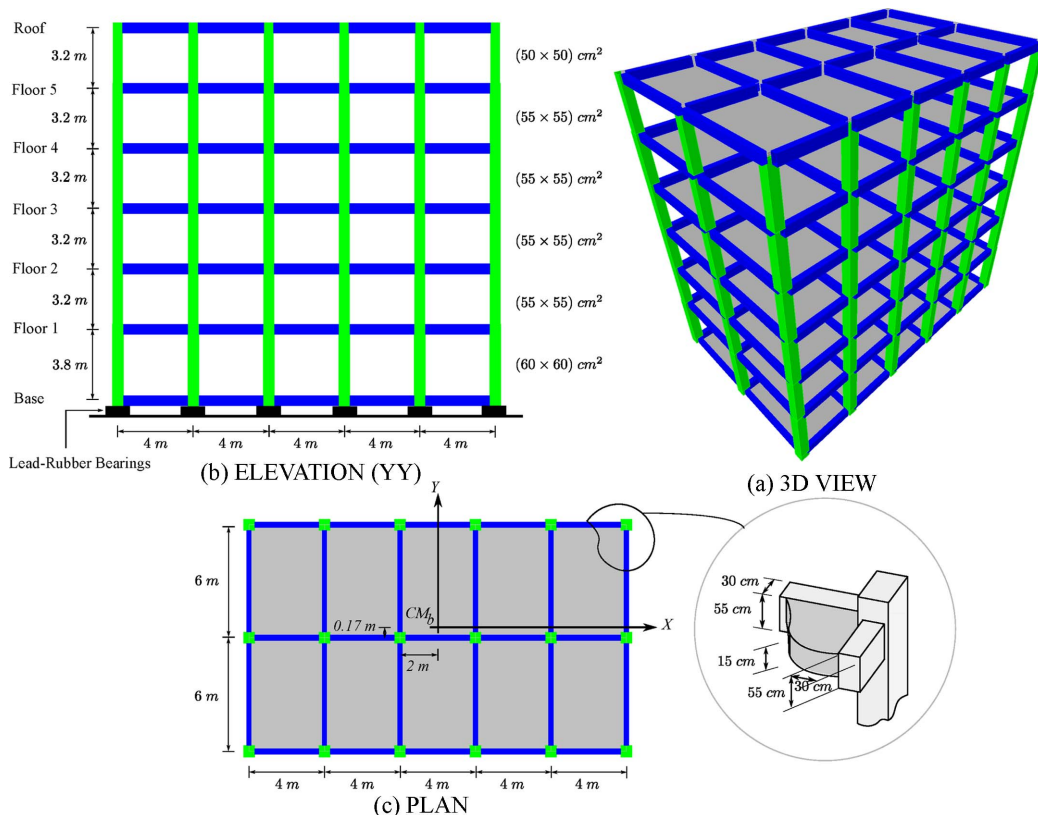


Fig. 5 Six-story reinforced concrete structure on LRB isolation system

Table 2 Selected components of CDMG suite of earthquakes

Earthquake	PGA (g)	PGV (cm/sec.)	PGD (cm)
El Centro 1979 (Array#6 station) 230°	0.436	108.709	55.165
Loma Prieta 1989 (Hollister station) 90°	0.178	30.891	20.418
Loma Prieta 1989 (Lexington Dam station) 90°	0.409	94.982	25.814
Landers 1992 (Lucerne valley station) Long	0.703	25.718	8.824
Northridge 1994 (Newhall station) 90°	0.583	74.841	17.595
Petrolia 1992 (Petrolia station) 90°	0.662	89.454	30.577
Northridge 1994 (Sylmar station) 90°	0.604	76.936	15.217
Landers 1992 (Yermo station) 360°	0.151	29.032	22.779

yield displacement x_y is set to 1 cm. The postyield stiffness is determined based on an isolation period T_b of 2 sec.

Eight records are selected from the CDMG (California Division of Mines and Geology, Sacramento, USA) suite of ground motions representing near fault effects, low and large ground velocities, which are specifically suggested by the CDMG for design of seismically isolated structures (Naeim and Kelly 1999). The records and their characteristics are summarized in Table 2. The superstructure is modeled as a three-dimensional shear structure. Lead-Rubber Bearings are modeled using biaxial model for elastomeric bearings to capture the interaction and keeping its effect on the seismic response (Park 1986). The dynamic response is computed for the selected accelerograms and the structure is subjected to each component in the X direction only, but keeping the biaxial interaction so that the response will be affected.

In the application of RSA-BI procedure the superstructure was simulated as lumped mass model (stick model) with condensed stiffness at each story calculated by summation of column stiffnesses in the X direction. The RSA-BI implies introduction of mass matrix, spectral, and modal matrices; they are given as below (units: kN, m, sec., rad):

$$M = \begin{bmatrix} 176.59 & 0 & 0 & 0 & 0 & 0 & 0 \\ 0 & 197.61 & 0 & 0 & 0 & 0 & 0 \\ 0 & 0 & 201.39 & 0 & 0 & 0 & 0 \\ 0 & 0 & 0 & 201.39 & 0 & 0 & 0 \\ 0 & 0 & 0 & 0 & 201.39 & 0 & 0 \\ 0 & 0 & 0 & 0 & 0 & 209.62 & 0 \\ 0 & 0 & 0 & 0 & 0 & 0 & 191.083 \end{bmatrix}$$

$$\Omega^2 = \begin{bmatrix} 9.874 & 0 & 0 & 0 & 0 & 0 & 0 \\ 0 & 13579.259 & 0 & 0 & 0 & 0 & 0 \\ 0 & 0 & 49129.860 & 0 & 0 & 0 & 0 \\ 0 & 0 & 0 & 98243.604 & 0 & 0 & 0 \\ 0 & 0 & 0 & 0 & 158261.570 & 0 & 0 \\ 0 & 0 & 0 & 0 & 0 & 215497.986 & 0 \\ 0 & 0 & 0 & 0 & 0 & 0 & 253309.931 \end{bmatrix}$$

$$\Phi = \begin{bmatrix} 0.02696 & 0.04034 & 0.04222 & 0.03280 & 0.01866 & 0.00936 & 0.00385 \\ 0.02696 & 0.02976 & 0.00215 & -0.02945 & -0.03840 & -0.02962 & -0.01499 \\ 0.02695 & 0.01656 & -0.02678 & -0.02924 & 0.01236 & 0.03801 & 0.02820 \\ 0.02694 & -0.00002 & -0.03591 & 0.01420 & 0.03368 & -0.01763 & -0.03611 \\ 0.02692 & -0.01659 & -0.01849 & 0.03665 & -0.02522 & -0.01610 & 0.03722 \\ 0.02690 & -0.02978 & 0.01260 & 0.00491 & -0.02406 & 0.03764 & -0.03133 \\ 0.02688 & -0.03552 & 0.03054 & -0.02804 & 0.02692 & -0.02383 & 0.01542 \end{bmatrix}$$

Note that the modal matrix is normalized with respect to the mass. The first term in the structure mass matrix represents the mass of the upper story while the last term corresponds to the base mass

Table 3 Peak response results of RSA-BI compared with NLTHA

Earthquake	Story	Force (kN)			Shear (kN)		
		RSA-BI	NLTHA	Error (%)	RSA-BI	NLTHA	Error (%)
Array#6	6	707.85	644.45	9.84	707.85	644.45	9.84
	5	787.93	720.28	9.39	1495.77	1364.7	9.6
	4	806.84	733.21	10.04	2302.62	2097.9	9.76
	3	806.51	732.11	10.16	3109.13	2830.1	9.86
	2	806.03	731.54	10.18	3915.16	3561.6	9.93
	1	838.64	761.43	10.14	4753.8	4323	9.97
	B	777.31	693.7	12.05	5531.11	5119.5	8.04
Hollister	6	216.32	206.32	4.85	216.32	206.32	4.85
	5	240.79	229.17	5.07	457.11	435.49	4.96
	4	246.47	235.04	4.91	703.68	670.53	4.94
	3	246.47	241.89	1.89	950.15	909.36	4.49
	2	246.32	251.88	-2.21	1196.48	1153.7	3.71
	1	256.29	262.41	-2.33	1452.77	1408.8	3.12
	B	237.55	227.8	4.28	1690.31	1636.6	3.28
Lexington	6	689.33	641.49	7.46	689.33	641.49	7.46
	5	767.31	720.26	6.53	1456.65	1360.1	7.1
	4	785.74	734.99	6.9	2242.38	2093.4	7.12
	3	785.41	733.64	7.06	3027.79	2822	7.29
	2	784.95	732.71	7.13	3812.74	3554.7	7.26
	1	816.7	765.16	6.74	4629.44	4319.8	7.17
	B	756.98	697.43	8.54	5386.42	5005.9	7.6
Lucerne	6	163.8	162.96	0.52	163.8	162.96	0.52
	5	182.33	183.51	-0.64	346.13	345.65	0.14
	4	186.71	187.51	-0.43	532.84	531.28	0.29
	3	186.63	185.44	0.64	719.47	711.62	1.1
	2	186.52	187.35	-0.44	905.99	889.63	1.84
	1	194.07	194.76	-0.36	1100.06	1084.4	1.44
	B	179.87	173.64	3.59	1279.93	1257.9	1.75

while the first term in the spectral matrix corresponds to the isolation system.

Tables 3 and 4 summarize the comparison between peak response values obtained by the NLTHA and those predicted by RSA-BI. Results of the tables are interpreted graphically in Fig. 6. Peak response values predicted by RSA-BI are close to those obtained using NLTHA with 12% as maximum error. Also, the RSA-BI predicted accurately the shape of peak floor forces distribution throughout the height of the structure; this demonstrates the use of Φ_{sup} and Ω_{sup}^2 instead of using modal and spectral matrices of the fixed base structure. However, using RSA-BI yields conservative estimates, this is due to the approximation used in uncoupling the equations of motion.

Neglecting floor accelerations relative to the base (Seguín *et al.* 2008), from Eq. (9) the shear force at story 1 above the base, which is the sum of all forces above the base, is

Table 4 Peak response results of RSA-BI compared with NLTHA (continued)

Earthquake	Story	Force (kN)			Shear (kN)		
		RSA-BI	NLTHA	Error (%)	RSA-BI	NLTHA	Error (%)
Newhall	6	418.46	385.64	8.51	418.46	385.64	8.51
	5	465.8	429.35	8.49	884.26	814.99	8.5
	4	476.98	437.16	9.11	1361.24	1252.1	8.72
	3	476.79	440.75	8.18	1838.03	1691.5	8.66
	2	476.5	445.82	6.88	2314.53	2135.4	8.39
	1	495.78	464.09	6.83	2810.31	2599.3	8.12
	B	459.53	417.42	10.09	3269.84	3016.7	8.39
Petrolia	6	671.76	639.89	4.98	671.76	639.89	4.98
	5	747.75	715.54	4.5	1419.52	1355.52	4.73
	4	765.71	724.81	5.64	2185.22	2080.2	5.05
	3	765.39	714.7	7.09	2950.62	2794.9	5.57
	2	764.94	706.73	8.24	3715.55	3501.7	6.11
	1	795.88	735.44	8.22	4511.44	4237.1	6.47
	B	737.68	676.51	9.04	5249.12	4913.6	6.83
Sylmar	6	688.83	624.9	10.23	688.83	624.9	10.23
	5	766.75	701.59	9.29	1455.58	1325.7	9.8
	4	785.16	715.94	9.67	2240.74	2041.5	9.76
	3	784.84	714.18	9.89	3025.58	2755.6	9.8
	2	784.37	711.65	10.22	3809.96	3467.2	9.89
	1	816.11	739.75	10.32	4626.06	4206.9	9.96
	B	756.43	675.47	11.99	5382.49	4882.4	10.24
Lucerne	6	238.16	227.85	4.53	238.16	227.85	4.53
	5	265.1	254.43	4.2	503.27	482.23	4.36
	4	271.47	258.3	5.1	774.73	740.5	4.62
	3	271.36	256.63	5.74	1046.09	997.13	4.91
	2	271.2	255.47	6.16	1317.29	1252.6	5.16
	1	282.17	265.99	6.08	1599.46	1518.6	5.32
	B	261.53	243.39	7.45	1860.99	1762	5.62

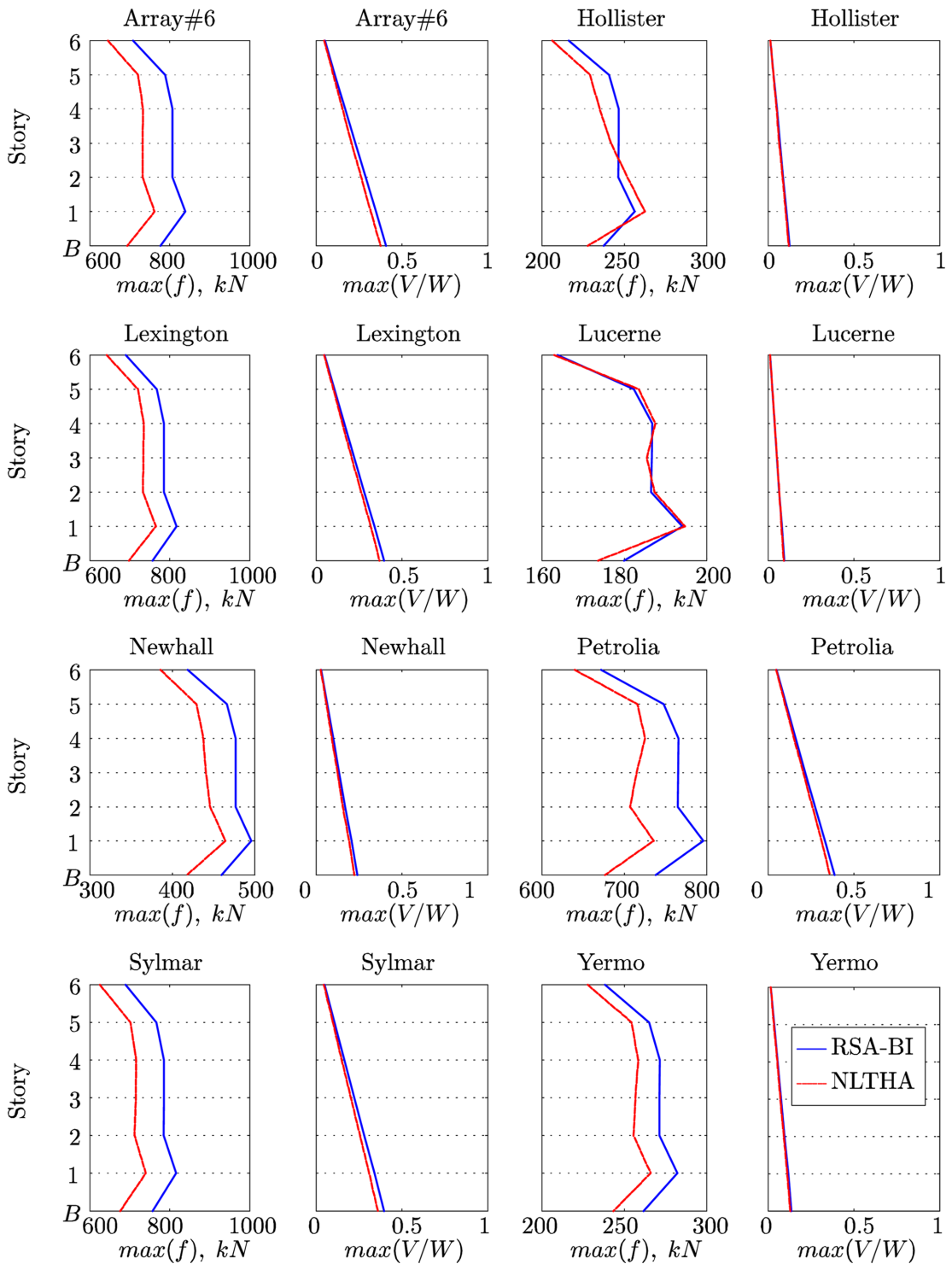


Fig. 6 Comparison of peak story forces and shear forces obtained by NLTHA and RSA-BI for the six-story structure

$$V_1 \approx M_{sup}(\ddot{u}_g(t) + \ddot{x}) \tag{13}$$

hence

$$V_1 \approx \frac{M_{sup} f_b}{m_b} \tag{14}$$

where f_b is the force mobilized at the base level. From Eq. (10) we have

$$V_1 + f_b = V_b \tag{15}$$

Substituting the value of f_b from Eq. (14) into Eq. (15) yields

$$V_b = V_1 \left(1 + \frac{m_b}{M_{sup}} \right) \tag{16}$$

Substituting $m_b = M_{tot} - M_{sup}$ into the Eq. (16) yields

$$\frac{V_b}{V_1} \approx \frac{M_{tot}}{M_{sup}} = \psi \tag{17}$$

As demonstrated by York and Ryan (2008), the superstructure to isolation frequency ratio (ω_d/ω_s) has a slight influence on the ratio V_b/V_1 . For base isolated structures with large damping ratios and smaller mass ratios (heavy bases) the $\psi \approx V_b/V_1$ approximation underestimates the shear force in the superstructure (York and Ryan 2008). However, a comprehensive search conducted by the author showed that the approximation $\psi \approx V_b/V_1$ remains a good estimation for most existent base isolated buildings.

In the present base-isolated structure the ratio $\psi = 1.161$. Fig. 7(a) shows the first story shear force to base shear ratio determined from RSA-BI and NLTHA versus $1/\psi$ ratio, it is clear that this ratio provides accurate results. In addition, Fig. 7(b) shows the story shear forces ratios, from the upper story to the base obtained from RSA-BI and NLTHA.

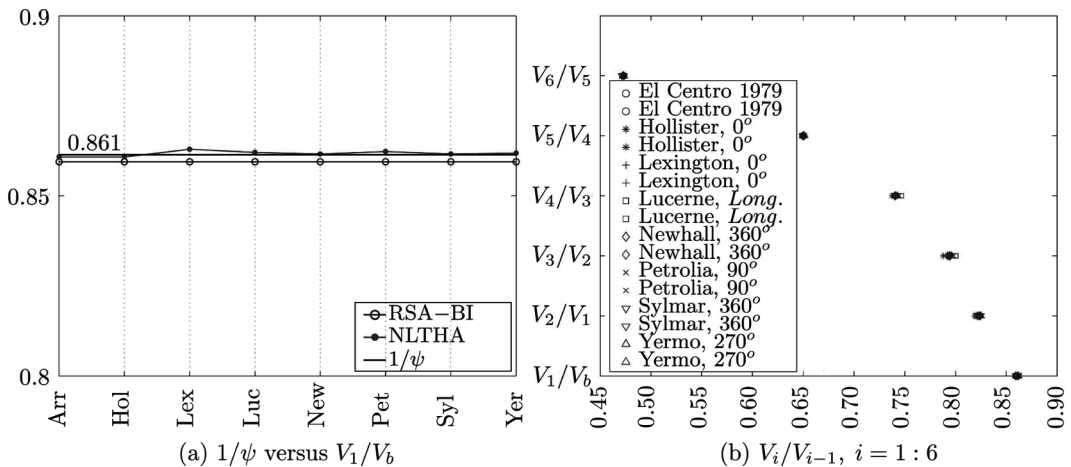


Fig. 7 Story shear forces ratios for the six-story structure subjected to the selected ground motions

5. Conclusions

This paper presents a response spectrum analysis procedure (RSA-BI) suitable for base isolated regular buildings subjected to near fault ground motions. The accuracy of the procedure has been verified with nonlinear dynamic analyses considering a selected set of near fault ground motions. It was shown that the RSA-BI might lead to conservative estimates of the building response, but within acceptable range.

As in any response spectrum analysis procedure, the applicability of the RSA-BI is restricted to base isolated regular buildings with limited number of stories. Nevertheless, the concept of RSA-BI is a promising tool for reliable design of base isolated buildings with bilinear hysteretic behavior. However, further research is needed to investigate the limitations of the proposed procedure.

Acknowledgements

This paper has been prepared based in part on the PhD thesis of the author conducted under the supervision of Professor Dan Lungu at the Technical University of Civil Engineering of Bucharest, Romania. The Scholarship provided by the Algerian Ministry of Higher Education and Scientific Research and Romanian State is acknowledged.

References

- Andriono, T. and Carr, A.J. (1991), "A simplified earthquake resistant design method for base-isolated multistory structures", *Bull. NZ. Natl. Soc. Earthq. Eng.*, **24**(3), 238-250.
- Andriono, T. and Carr, A.J. (1991), "Reduction and distribution of lateral seismic inertia forces on base-isolated multistory structures", *Bull. NZ. Natl. Soc. Earthq. Eng.*, **24**(3), 225-237.
- Cardone, D., Dolce, M. and Guesaldi, G. (2009), "Lateral force distributions for the linear static analysis of base-isolated buildings", *Bull. Earthq. Eng.*, **7**(3), 801-834.
- Çelebi, M. (1996), "Successful performance of a base-isolated hospital building during the 17 January 1994 Northridge earthquake", *Struct. Design Tall Build.*, **5**(2), 95-109.
- Chopra, A.K. (2005), *Dynamics of Structures Theory and Applications to Earthquake Engineering*, Prentice Hall, NJ.
- Deb, S.K., Paul, D.K. and Thakkar, S.K. (1997), "Simplified non-linear dynamic analysis of base isolated buildings subjected to general plane motion", *Eng. Comput.*, **14**(5), 542-557.
- Jangid, R.S. (2002), "Parametric study of base isolated structures", *Adv. Struct. Eng.*, **5**(2), 113-122, Multiscience Publishing Co. Ltd., London, UK.
- Jangid, R.S. (2007), "Optimum lead-rubber isolation bearings for near-fault motions", *Eng. Struct.*, **29**(10), 2503-2513.
- Jangid, R.S. and Kelly, J.M. (2001), "Base isolation for near-fault motions", *Earthq. Eng. Struct. Dyn.*, **30**(5), 691-707.
- Lee, D.G., Hong, J.M. and Kim, J. (2001), "Vertical distribution of equivalent static loads for base isolated building structures", *Eng. Struct.*, **23**(10), 1293-1306.
- Makris, N. and Chang, S.P. (2000), "Effect of viscous, viscoplastic, and friction damping on the response of seismic isolated structures", *Earthq. Eng. Struct. Dyn.*, **29**(1), 85-107.
- Matsagar, V.H. and Jangid, R.S. (2004), "Influence of isolator characteristics on the response of base-isolated structures", *Eng. Struct.*, **26**(12), 1735-1749.
- Mokha, A., Constantinou, M.C. and Reinhorn, A.M. (1988), *Teflon Bearings in Aseismic Base Isolation*:

- Experimental Studies and Mathematical Modeling*, Technical Report NCEER-88-0038, State University of New York, Buffalo, NY.
- Moussa, L. (2009), *Base Isolated Buildings: Parametric Dynamic Analysis and Computer Simulations*, Ph.D. Thesis, Technical University of Civil Engineering, Bucharest, Romania.
- Naeim, F. and Kelly, J.M. (1999), *Design of Seismic Isolated Structures: From Theory to Practice*, John Wiley and Sons, Inc., NY.
- Nagarajaiah, S., Reinhorn, A.M. and Constantinou, M.C. (1991), "Nonlinear dynamic analysis of 3D-base isolated structures", *J. Struct. Eng.*, **117**(7), 2035-2054.
- Nagarajaiah, S., Reinhorn, A.M. and Constantinou, M.C. (1993), "Torsion in base isolated structures with elastomeric isolation systems", *J. Struct. Eng.*, **119**(10), 2932-2951.
- Narasimhan, S., Nagarajaiah, S., Johnson, A. and Gavin, H.P. (2003), "Smart base isolated building benchmark problem", *Proceedings of 16th ASCE Engineering Mechanics Conference*, University of Washington, Seattle.
- Newmark, N.M. and Hall, W.J. (1982), *Earthquake Spectrum and Design*, Monograph Series, Earthquake Engineering Research Institute, Oakland.
- Park, Y.J., Wen, Y.K. and Ang, A.H.S. (1986), "Random vibration of hysteretic systems under bi-directional ground motions", *Earthq. Eng. Struct. D.*, **14**(4), 543-557.
- Reinhorn, A.M., Nagarajaiah, S., Constantinou, M.C., Tsopelas, P. and Li, R. (1994), *3D-BASIS: Version 2.0 Computer Program for Nonlinear Dynamics Analysis of Three Dimensional Base Isolated Structures*, Technical Report NCEER-95-0018, State University of New York, Buffalo, NY.
- Ribakov, Y. (2010), "Reduction of structural response to near fault earthquakes by seismic isolation columns and variable friction dampers", *Earthq. Eng. Eng. Vib.*, **9**(1), 113-122.
- Ryan, K.L. and Chopra, A.K. (2004), "Estimation of seismic demands on isolators in asymmetric buildings using non-linear analysis", *Earthq. Eng. Struct. D.*, **33**(3), 395-418.
- Ryan, K.L. and Chopra, A.K. (2005), *Estimating The Response of Base Isolated Buildings Including Torsion, Rocking and Axial Load Effects*, Report No. UCB/EERC 2005-01, Earthquake Engineering Research Center, Berkeley, CA.
- Ryan, K.L. and Chopra, A.K. (2006), "Estimating seismic demands for isolation bearings with building overturning effects", *J. Struct. Eng. ASCE*, **132**(7), 1118-1128.
- Seguin, C.E., De la Llera, J.C. and Almazan, J.L. (2008), "Base structure interaction of linearly isolated structures with lateral torsional coupling", *Eng. Struct.*, **30**(1), 110-125.
- Stanton, J.F. and Roeder, C.W. (1991). "Advantages and Limitations of Seismic Isolation", *EERI Spectra*, **7**(2), 301-309.
- Tena-Colunga, A. (2002), "Seismic design of base-isolated structures using constant strength spectra", *J. Earthq. Eng.*, **6**(4), 553-585.
- Tsai, C.S., Chen, B.J. and Chiang, T.C. (2003), "Experimental and computational verification of reasonable design formulae for base-isolated structures", *Earthq. Eng. Struct. D.*, **32**(9), 1389-1406.
- Tsai, C.S., Chen, W.S., Chen, B.J. and Pong, W.S. (2006), "Vertical distributions of lateral forces on base isolated structures considering higher mode effects", *Struct. Eng. Mech.*, **23**(5), 543-562.
- Wen, Y.K. (1976), "Method of random vibration of hysteretic systems", *J. Eng. Mech. Div.*, **102**(2), 249-263.
- York, K. and Ryan, K.L. (2008), "Distribution of lateral forces in base-isolated buildings considering isolation system nonlinearity", *J. Earthq. Eng.*, **12**(7), 1185-1204.
- Zayas, V.A., Low, S.S., Bozzo, L.M. and Mahin, S.A. (1989), *Feasibility and Performance Studies on Improving The Earthquake Resistance of New and Existing Buildings Using The Friction Pendulum System*, Report No. UCB/EERC-89/09, Earthquake Engineering Research Center, Berkeley, CA.